Ultrasonics 94 (2019) 305–313

Contents lists available at ScienceDirect

Ultrasonics

journal homepage: www.elsevier.com/locate/ultras

Effect of vibration frequency and displacement on melt expulsion characteristics and geometric parameters for ultrasonic vibration-assisted laser drilling of steel

S. Habib Alavi, Sandip P. Harimkar*

School of Mechanical and Aerospace Engineering, Oklahoma State University, Stillwater, OK 74078, United States

ARTICLE INFO

Keywords:
Ultrasonic vibrations
Laser drilling
Material removal
Melt expulsion

ABSTRACT

Recently, the applications of ultrasonic vibration assistance to laser-based manufacturing processes are rapidly proliferating. Ultrasonic vibration-assisted laser drilling (UVLD) process involves simultaneous application of high frequency vertical vibrations to the workpiece while being irradiated with a continuous wave laser beam. In UVLD, the ultrasonic vibration assistance causes expulsion of droplets from the laser melted surface, resulting in the formation of deep holes. In this paper, systematic analysis of the effects of ultrasonic vibration frequency (20–40 kHz) and displacement (16–32 μm) on melt expulsion characteristics in early stages of drilling and geometric/quality features of the holes for UVLD of AISI 316 is presented. Based on the analysis of initiation of droplet ejection from the melt pool and particle size of the ejected droplets, mechanisms of droplet ejection based on capillary wave theory are proposed. It was observed that while increasing both ultrasonic vibration frequency and displacement resulted in reduction in droplet ejection initiation time and the formation of deeper holes for the given laser irradiation time (100 ms), the effect of vibration displacement was much more pronounced than the frequency on the variation.

1. Introduction

Conventional materials processing and manufacturing technologies have undergone continuous improvements and new technologies have been regularly developed to address several challenges related to productivity, process efficiency, part complexity and quality, scalability, materials compatibility, and manufacturing economics. Recently, applications of ultrasonic vibrations in materials processing are rapidly expanding to further improve the outcomes of conventional processes or enable additional manufacturing flexibility [1–5]. While ultrasonic vibrations have established applications in materials cleaning, sonochemistry, liquid metal processing [6], atomization [7], and plastic and metals welding [8,9], their applications as an assistance or aid to advanced manufacturing processes such as precision machining [10,11], welding [12], laser processing [13,14], and additive manufacturing [15,16] are rapidly proliferating. These ultrasonic vibration-assisted manufacturing processes offer several advantages over the conventional processes. The outcomes of these processes depend not only on the primary process parameters but also on ultrasonic parameters namely vibration frequency and amplitude. However, the effect of these ultrasonic parameters on the process outcomes is not well investigated for these emerging ultrasonic vibration-assisted manufacturing processes.

The effects of ultrasonic vibration assistance to conventional machining processes such as drilling on machining characteristics (machining force, chip morphology, workpiece quality, and tool wear) are widely investigated for difficult-to-machine materials. Liao et al. [17] investigated ultrasonic vibration-assisted drilling of Inconel 718 superalloy with a range of vibration parameters (amplitudes of 4–12 and 8–17 μm at vibration frequencies of 31.8 and 20.3 kHz, respectively). It was reported that ultrasonic vibration assistance resulted in general reduction in chip size, increase in proportion of segmented chips, reduction in thrust force, and increase in tool life. The effect of vibration amplitude was observed to be more pronounced than the frequency on the machining characteristics, leading to the conclusion that high frequency and small amplitude vibrations give better results for ultrasonic vibration-assisted drilling of the superalloys. Azarhoushang and Akbari [18] also reported that multiple impact interaction between tool and workpiece during ultrasonic vibration-assisted drilling (frequency of 21 kHz and amplitude of 10 μm) resulted in the formation of discontinuous finer chips for Inconel 738-LC alloy, resulting in overall improvement in surface finish and tool life. Kadivar et al. [19] also

* Corresponding author.
E-mail address: sandip.harimkar@okstate.edu (S.P. Harimkar).

https://doi.org/10.1016/j.ultras.2018.08.012
Received 10 January 2018; Received in revised form 1 June 2018; Accepted 16 August 2018
Available online 17 August 2018
0041-624X/

investigated the effect of ultrasonic parameters (frequency of 22 kHz and amplitudes of 5–15 μm) on the machining characteristics for ultrasonic vibration-assisted drilling of Al/SiC_p metal matrix composites. It was observed that the ultrasonic vibrations of lower amplitudes resulted in higher improvements in machining performance measured in terms of surface finish and burr height. The effect of ultrasonic parameters (frequency 10–30 kHz and amplitude 5–25 μm) on the chip morphology and machining forces was also investigated for ultrasonic vibration-assisted drilling of cortical bone by Alam et al. [20]. The machining force and torque for the ultrasonic vibration-assisted drilling were significantly lower than that for conventional drilling. For the ultrasonic vibration-assisted drilling, the machining force showed continuous reduction with increasing frequency from 10 to 30 kHz (for the constant amplitude of 10 μm) while the significant reduction in force was observed with increasing vibration amplitude from 5 to 15 μm (for the constant frequency of 20 kHz). Further increase in vibration amplitude from 15 to 25 μm did not result in any additional improvement in machining force. Clearly, most of these studies on ultrasonic vibration-assisted drilling reported improved chip removal and reduction in forces for a range of materials. These studies also demonstrated that high frequency and small amplitude ultrasonic vibrations offer optimum improvements in machining performance for the ultrasonic vibration-assisted drilling.

Recently, the application of ultrasonic vibration assistance in laser-based manufacturing processes such as additive manufacturing, surface melting, and drilling is attracting significant attention. Cong and Ning [21] investigated the influence of the application of vertical vibrations of frequency 41 kHz to the substrate during direct energy deposition (DED) based laser additive manufacturing of AISI 630 stainless steel. It was observed that the ultrasonic vibration assistance during additive manufacturing improves powder efficiency, alleviates balling effect, reduces defects (cracks and porosity), and refines the grain structure of the built parts. Hu et al. also studied the influence of ultrasonic vibration assistance during laser engineering net shaping of ZrO_2-Al_2O_3 specimens on crack suppression tendency, microstructure, and mechanical properties [22]. They reported grain refinement and suppression of crack initiation and propagation in specimens fabricated using ultrasonic vibration-assisted laser engineered net shaping. Ning et al. also investigated the simultaneous application of the ultrasonic vibrations during laser engineering net shaping of Inconel 718 specimens [23]. It was observed that the application of ultrasonic vibrations assistance during laser processing decreases the mean porosity and refines the microstructure. The effects such as cavitation and acoustic streaming due to ultrasonic vibrations, also observed in liquid metal processing, are likely the causes of desired metallurgical effects observed for ultrasonic vibration-assisted additive manufacturing. Biswas et al. [24] also observed similar grain refinement effects due to ultrasonic vibration assistance (frequency of 20 kHz) to laser melting of Ti-6Al-4V. In these studies [21,24], vertical ultrasonic vibrations are applied directly to substrate while being irradiated with relatively defocused laser beam for melting or deposition. However, Biswas et al. [24] also reported that the application of intense ultrasonic vibrations to the substrate during laser melting cause some expulsion of molten material from the melt pool, creating surface craters upon solidification. The melt expulsion characteristics during ultrasonic vibration-assisted laser melting of AISI 316 stainless steel was investigated by Alavi and Harimkar [25]. It was observed that the application of ultrasonic vibrations (frequency of 20 kHz and displacements 23–51 μm) during laser melting delayed the interaction of laser with the material due to enhanced convection effects and caused expulsion of melt from the pool. For the given laser irradiation time, increasing ultrasonic vibration displacements resulted in shallower craters with a thinner resolidified layer, indicating higher convection enhancement and effective melt expulsion at higher displacements. Alavi and Harimkar [26] further investigated the feasibility of utilizing the observations of melt expulsion during ultrasonic vibration-assisted laser melting for designing material removal processes. They reported that the application of ultrasonic vibrations (frequency 20 kHz and displacements 23–51 μm) to the AISI 316 stainless steel substrate during laser surface melting with a focused laser beam results in significant melt expulsion from the substrate, creating deep holes (up to 1.5 mm with an aspect ratio of about 3.5). The depth of hole continuously increased with increasing ultrasonic displacement for the proposed ultrasonic vibration-assisted laser drilling (UVLD) of steel. Alavi and Harimkar [27,28] further investigated the effect of laser processing parameters (irradiation time and focusing conditions) on the geometric and quality aspects of the holes drilled in AISI 316 stainless using UVLD. While most of these studies reported beneficial effects of the simultaneous application of ultrasonic vibrations during laser-based manufacturing processes (additive manufacturing, melting, and drilling), systematic investigations on the effects of vibration parameters on the process outcomes were not performed.

In this paper, systematic effect of ultrasonic vibration frequency (20–40 kHz) and displacement (16–32 μm) on the melt expulsion characteristics in early stages of UVLD of AISI 316 is investigated using high speed camera imaging. Based on the analysis of initiation of droplet ejection from the melt pool and particle size of ejected droplets, mechanisms of droplet ejection based on capillary wave theory are proposed. Furthermore, the effect of ultrasonic vibration parameters on the development of geometric and quality features of the holes drilled with UVLD is analyzed.

2. Experimental procedure

UVLD setup consisted of an ultrasonic vibration generator (Vibra-Cell Series, Sonics & Materials, Inc, Newtown, CT) and a continuous wave CO_2 laser (MF 1500, Ferranti, Manchester, UK). The details of the experimental setup are shown in Fig. 1. The drilling experiments were performed on commercial AISI 316 stainless steel specimens. The steel samples were machined to 3.5 mm thickness, followed by polishing and sand blasting to improve the laser beam absorption. The samples were then mounted on 13 mm diameter titanium alloy probe/horn of the ultrasonic system. The ultrasonic generators were operated to produce vertical vibrations of displacements 16, 24, and 32 μm at the sample surface at each vibration frequency (20 and 40 kHz). The CO_2 laser was operated at power of 900 W with the beam diameter of 0.8 mm (corresponding to the working distance of 5 mm). The vibrations were applied to the samples during the entire duration of laser irradiation time (t_I = 100 ms). Argon shielding gas was used to prevent surface

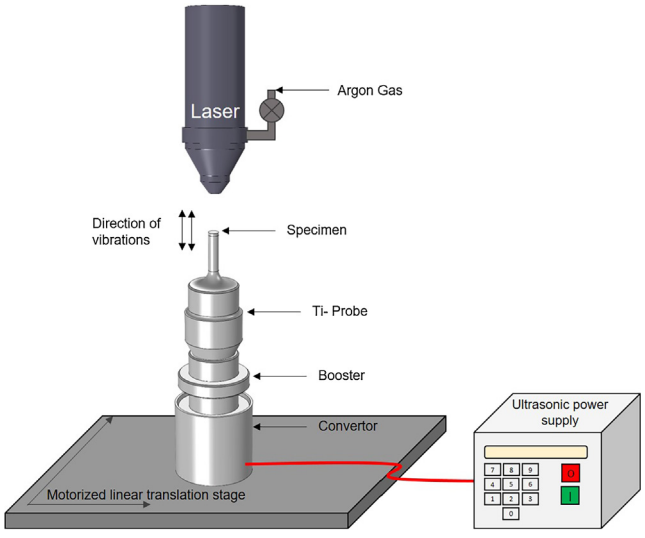

Fig. 1. Schematic of the experimental setup for ultrasonic vibration-assisted laser drilling (UVLD).

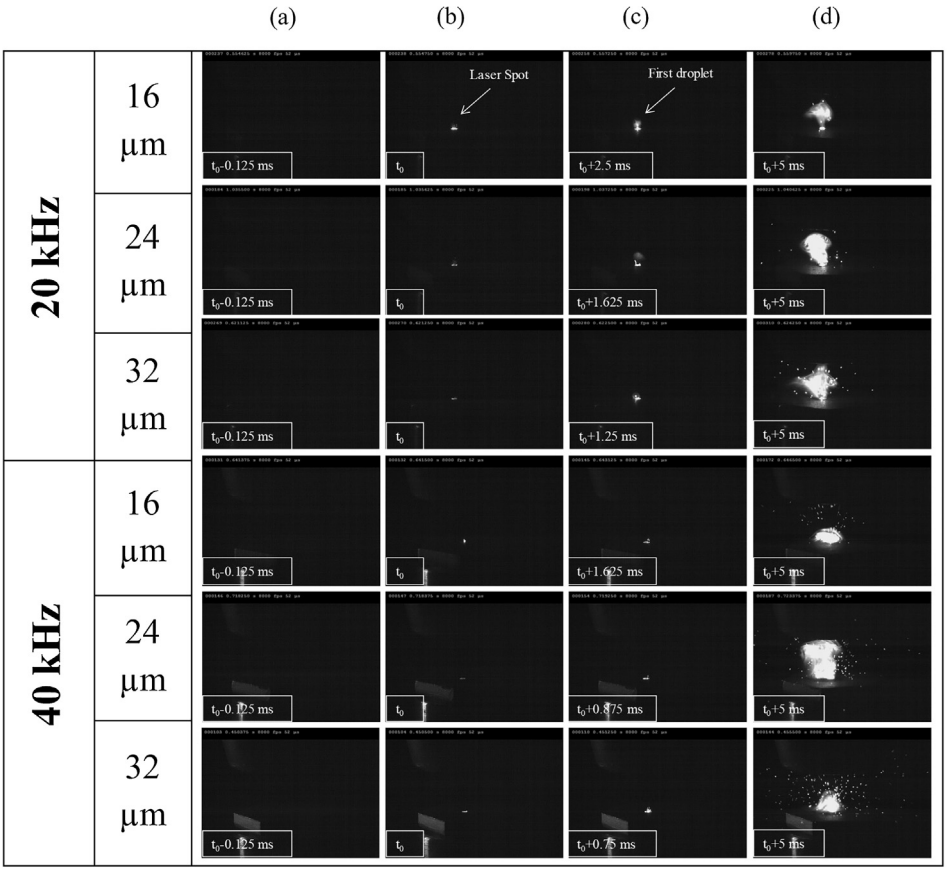

Fig. 2. High speed camera images showing: (a and b) initiation of laser interaction, (c) first droplet ejection, and (d) continued ejection of droplets during UVLD of AISI 316 steel for ultrasonic vibration displacements of 16, 24, and 32 µm at frequencies of 20 and 40 kHz.

oxidation during laser drilling. A high speed camera (XS-4, Integrated Design Tools, Inc, Tallahassee, FL), operating at the frame rate (frames/s) of 8000, was used to capture images of droplet ejection from the melt pool during early stages of drilling. A scanning electron microscope (JSM-6360, JEOL Ltd, Tokyo, Japan) was used to image features on surface and cross-sections of the laser drilled holes. A public domain image processing software, Image J, was used to measure the geometric and quality features of the laser drilled holes from the SEM micrographs. A three-dimensional optical surface profiler (PS50, Nanovea, Irvine, CA) was used to measure the build-up volume of the material around the laser drilled hole periphery.

3. Results and discussion

3.1. Analysis of droplet ejection mechanisms during UVLD

3.1.1. High speed imaging of UVLD process

Fig. 2 shows the selected sequence of the frames capturing the major incidents during UVLD of stainless steel performed with ultrasonic vibration displacements of 16, 24, and 32 µm at the vibration frequencies of 20 and 40 kHz. The irradiation of laser on the vibrating surface causes surface heating and eventual melting of the substrate. For all the investigated parameters, the first two frames (Fig. 2a and b), captured at the spacing of 0.125 ms, show the first sign of transition to laser-interaction regime, indicated by the appearance of the bright spot on the surface of the substrate. The time corresponding to the second frame was considered the initiation of laser irradiation (t_0). This was also confirmed from the fact that the time from this frame to the last frame showing laser interaction corresponds exactly to the irradiation time used in this investigation (t_I = 100 ms). The continued laser irradiation beyond t_0 causes laser heating and melting. The melt pool remains stable until it reaches a certain minimum volume, referred to as critical volume of melt pool, before the initiation of droplet ejection from the surface of melt pool (Fig. 2c). Once the melt pool reaches the critical size, the destabilizing effects of the ultrasonic vibrations overcome the surface tension and gravitational forces, breaking the melt pool into fine droplets. From the high speed camera images, it is difficult to identify the initiation of melting i.e. the transition from heating to melting ($t = t_m$). The time corresponding to the initiation of droplet ejection (t_d) for the investigated processing parameters is also indicated on the frames. Depending on the ultrasonic vibration parameters (displacement and frequency), the droplet ejection from the laser melted pool begins at about 0.75–2.5 ms during laser irradiation. The droplet expulsion in the form of a stream continues during the entire duration of remaining laser irradiation time (Fig. 2d). From the observations of the high speed camera images, the proposed sequence of events leading to the formation of hole during UVLD is shown in Fig. 3.

The variation of droplet ejection initiation time (t_d) with ultrasonic vibration displacements at the vibration frequencies of 20 and 40 kHz is shown in Fig. 4. Clearly, for both ultrasonic vibration frequencies, the droplet ejection initiation time decreases with increasing ultrasonic vibration displacement from 16 to 32 µm. Furthermore, the droplet ejection initiation time at all vibration displacement is much shorter for vibration frequency of 40 kHz when compared to 20 kHz. The effect of vibration displacement is much more dominant than vibration frequency on the reduction in droplet ejection initiation time. For example, doubling the ultrasonic vibration displacement from 16 to 32 µm causes about 53% and 50% reduction in droplet ejection initiation time for vibration frequencies of 20 and 40 kHz, respectively. The effect of frequency on the droplet ejection initiation time progressively diminishes with increasing ultrasonic vibration displacement. The doubling of vibration frequency from 20 to 40 kHz results in about 39%

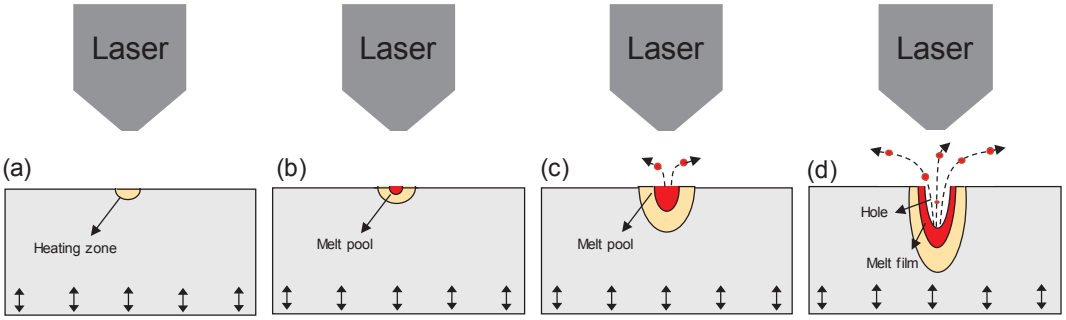

Fig. 3. Schematic of the sequence of events leading to the formation of hole during UVLD: (a) initiation of laser heating ($t = t_0$), (b) initiation of laser melting ($t = t_m$), (c) formation of critical volume of melt pool for the initiation of droplet ejection ($t = t_d$), and (d) continued ejection of a stream droplets during continued laser irradiation (*up to* $t = t_l$).

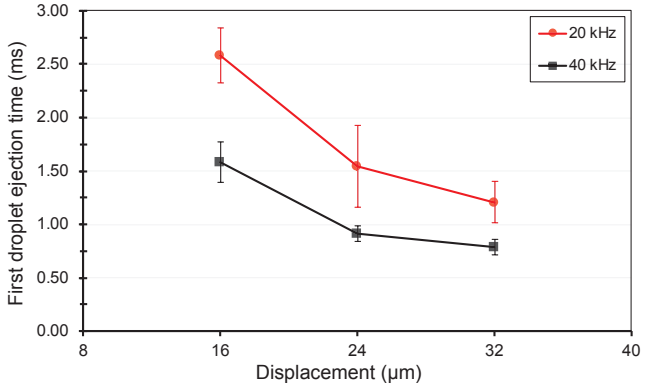

Fig. 4. Variation of droplet ejection initiation time with ultrasonic vibration displacement for vibration frequencies of 20 and 40 kHz during UVLD of AISI 316 steel.

and 34% reduction in droplet ejection initiation time for vibration displacements on 16 and 32 μm, respectively. At a given vibration frequency, the higher vibration displacement provides higher vertical speed and consequently higher acceleration to the substrate being laser melted at the surface. Higher vibration frequency at given displacement also means higher number of vibration cycles are applied to the melt pool per unit time. It can be concluded that the ultrasonic vibrations of higher vibration displacement and frequency impart higher destabilizing force on the melt pool causing earlier ejection of the droplets from the melt pool. However, it must be noted that the simultaneous application of ultrasonic vibrations to the substrate significantly modifies the heat transfer processes. It has been reported that the ultrasonic vibrations cause enhancement of surface convection both in air and liquid media [29,30]. Depending on the ultrasonic vibration parameters and system configuration, an increase in convection coefficients up to 25 times has been reported due to ultrasonic vibration assistance. In laser materials processing, the overall heat balance at the laser irradiated surface is determined by the absorbed laser energy at the surface and convective and radiative heat losses from the surface and is given by the heat transfer equation [31]:

$$-k\left[\left(\frac{\partial T}{\partial x}\right)+\left(\frac{\partial T}{\partial y}\right)+\left(\frac{\partial T}{\partial z}\right)\right]=\delta I_0-\varepsilon\sigma_{sb}\left[T^4-T_0^4\right]-h\left[T-T_0\right] \quad (1)$$

where k is the thermal conductivity (W/m K), δ is the absorptivity, I_0 is the incident laser intensity (W/m^2), ε is the emissivity, σ_{sb} is the Stefan-Boltzmann constant (W/m^2 K^4), and h is the convective heat transfer coefficient (W/m^2 K). The enhancement of surface convection, and consequent loss of energy, is also expected during simultaneous application of ultrasonic vibrations during laser irradiation in early stages of UVLD. The enhanced surface convection observed for UVLD can significantly modify the temperature distributions in the substrate compared to conventional laser processing without any assistance of ultrasonic vibration assistance. It is expected that the distributions would shift to lower temperatures for the UVLD case. The quantification of such thermal effects using finite element analysis requires estimation of air velocity and heat transfer coefficients. Consistent with the literature, it is expected that the enhancement of surface convection effects will increase with increasing severity of the ultrasonic vibrations as defined by higher vibration displacement and frequency. The higher convective losses from the laser irradiated surface during UVLD would then cause delays in critical laser interactions such as initiation of surface melting. In fact, it was reported [25] that the application of ultrasonic vibrations of frequency 20 kHz to the AISI 316 steel substrate during laser surface irradiation completely eliminates the possibility of surface melting with the similar laser processing parameters (laser power of 900 W, irradiation time of 0.30 s, and laser beam diameter of 7 mm) that cause surface melting of the substrate without the application of ultrasonic vibrations. Only heat affected zone was observed for the samples when they were laser irradiated with simultaneous application of ultrasonic vibrations to the samples. It was also reported that the size of the heat affected zone decreases and the heat affected zone eventually diminishes as the displacement of vibrations increases with the similar laser processing parameters and vibration frequency. Clearly, the enhancement of surface convection during UVLD is likely to cause increasing delays in laser surface interaction effects such as surface melting with increasing ultrasonic vibration displacement and vibration frequency. However, as observed from the high speed camera imaging, the droplet ejection initiation time during UVLD decreases with increasing ultrasonic vibration displacement and vibration frequency. It appears that even with stronger surface convection enhancement effects and consequent delays in surface melting, the higher destabilizing force offered by the higher ultrasonic vibration displacement and vibration frequency to the melt pool eventually causes the early ejection of droplets from the melt pool during UVLD. The critical volume of the melt pool for the initiation of droplet ejection is also likely to be much smaller at higher ultrasonic vibration displacement and frequency during UVLD.

3.1.2. *Analysis of ejected particles for UVLD*

To further understand the melt ejection mechanisms during UVLD, the size and distribution of the solidified droplets/particles were analyzed (Fig. 5). The particles ejected during UVLD at all the processing parameters were highly spherical and showed dendritic surface morphology, indicating rapid solidification of droplets in-flight. It was observed that the particle size distribution was relatively narrower for ultrasonic vibration frequency of 40 kHz at all the investigated vibration displacement. Also, the ejected particles were relatively smaller for the 40 kHz at the given ultrasonic vibration displacement. The average particle size for all the processing parameters is listed in Table 1. The average particle size was in the ranges of about 77–90 μm and 49–55 μm for the ultrasonic vibration frequencies of 20 and 40 kHz,

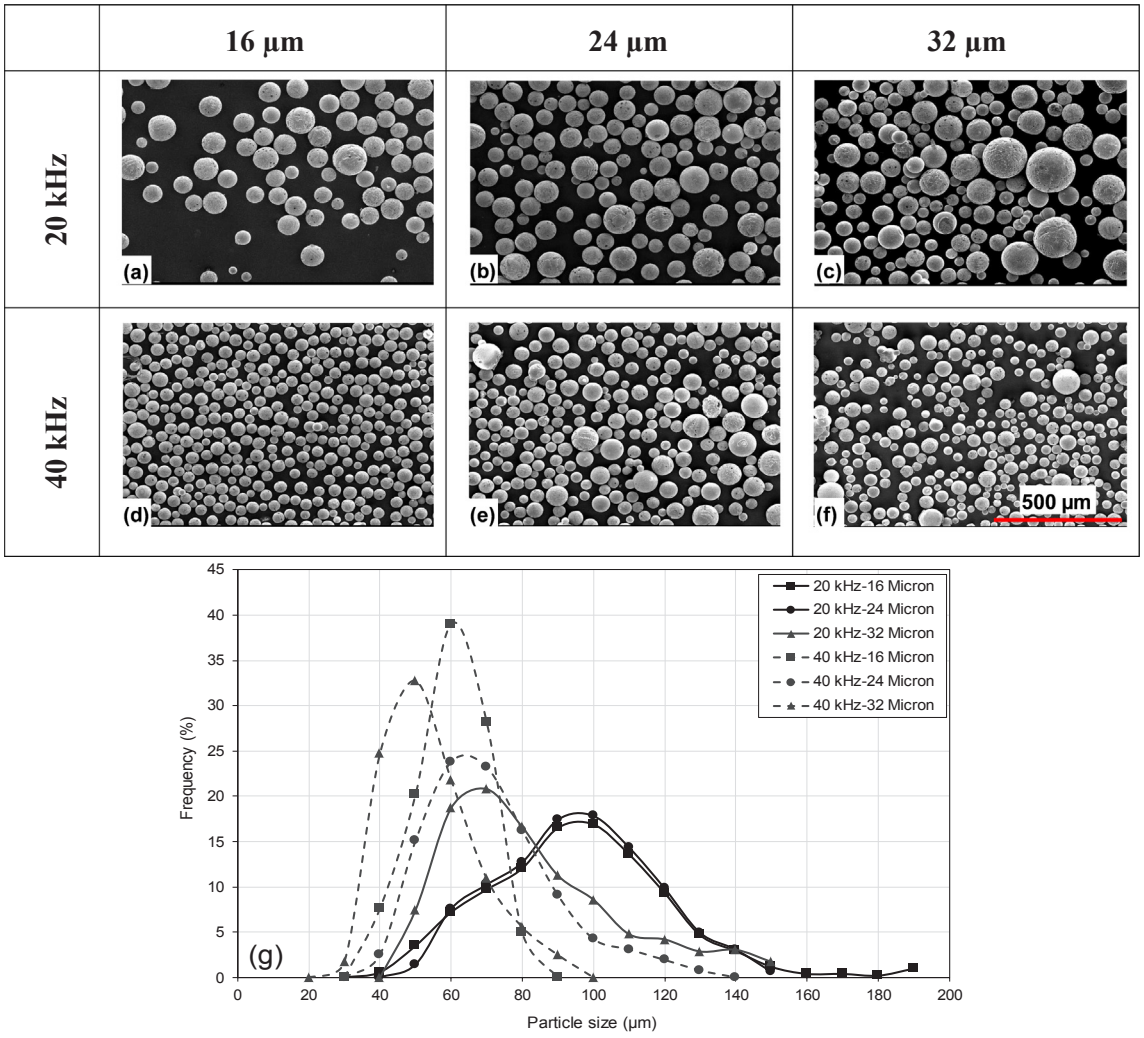

Fig. 5. (a–f) SEM micrographs of ejected particles and (g) size distributions of particles ejected during UVLD of AISI 316 steel for ultrasonic vibration displacements of 16, 24, and 32 µm at frequencies of 20 and 40 kHz.

Table 1
Theoretical and experimental sizes of ejected droplets during UVLD of AISI 316 steel.

Vibration frequency (kHz)	Vibration displacement (µm)	Experimental particle size (µm)	Theoretical particle size (µm)
20	16	90.0 ± 21.3	85.7
	24	84.5 ± 24.7	
	32	77.2 ± 24.0	
40	16	55.2 ± 9.5	54.0
	24	66.2 ± 17.6	
	32	49.1 ± 13.0	

respectively. The effect of ultrasonic vibration frequency was much more pronounced on the average particle size. The early stage ejection of droplets during UVLD is likely to be due to mechanisms very similar to capillary wave mechanisms during ultrasonic atomization of materials. In ultrasonic atomization, the liquid film of uniform thickness on the vibrating surface becomes unstable and forms ripples (capillary wave). During atomization, the amplitude of the capillary wave increases and the peaks of the wave break from the liquid film forming droplets. The wavelength of the capillary wave, taking into account main parameters of the atomization process, has been established based on Navier-Stokes analysis of film stability and is given by [32]:

$$\frac{2}{\pi f^2 \lambda_s}\left(4\frac{\sigma\pi^2}{\rho\lambda_s{}^2}+g\right)\tanh\left(\frac{2\pi l_m}{\lambda_s}\right)+0.02\left[\frac{\pi a_0}{\lambda_s}\tanh\left(\frac{2\pi l_m}{\lambda_s}\right)\right]^{1/2}-1.04=0 \quad (1)$$

where g, l_m, a_0, σ, ρ, and f are gravitational acceleration (m/s^2), liquid film thickness (m), and vibration amplitude (m), surface tension of the liquid (J/m^2), density of the liquid (kg/m^3), and frequency of ultrasonic vibrations (Hz), respectively. For very thin liquid film ($\tanh\left(\frac{2\pi lm}{\lambda_s}\right)\cong 1$), the impact of gravitational force is negligible compared to the ultrasonic force and the above equation reduces to the Lang's equation [7]:

$$\lambda_s=\left(\frac{8\pi\sigma}{\rho f^2}\right)^{1/3} \quad (2)$$

It has been further reported that the average diameter of the ejected droplets during ultrasonic atomization is predictable and is about 0.34 times the wavelength of the capillary wave (λ_s). The average particle size (D) for the ultrasonic atomization is given by:

$$D=0.34\left(\frac{8\pi\sigma}{\rho f^2}\right)^{1/3} \quad (3)$$

Assuming that the capillary wave hypothesis is applicable in the case of UVLD, this equation can be used to estimate the average particle size using thermo-physical properties of AISI 316 stainless steel at melting temperature (σ: 1.77 J/m^2 [33], ρ: 6950 kg/m^3 [34]). The average

particle size was calculated to be 85.7 and 54 μm for vibration frequencies of 20 and 40 kHz, respectively. It must be noted that the thickness of the liquid film in ultrasonic atomization is uniform while the laser irradiation on the surface with Gaussian beam forms semi-ellipsoidal melt pool with the highest depth at the center of the pool. Such non-uniform depth of the melt pool is likely to cause capillary waves of varying wavelengths, resulting in ejection of droplets over a wider size distribution as observed. Also, the laser melted pool always exhibits a temperature distribution with highest temperature at the surface, and the surface temperature of the melt pool often exceeds the melting temperature. It should be noted that the Lang's equation (Eq. (3)) considers only ultrasonic vibration frequency and material properties to predict the atomized particle size; the effect of ultrasonic vibration displacement is not taken into account in this prediction. The authors have previously used Navier-Stokes analysis (Eq. (1)) to estimate the effect of ultrasonic vibration displacement on the particle size for the ultrasonic vibration-assisted atomization of steel and showed that vibration displacement has no effect on estimated particle size consistent with Lang's analysis [35]. Nevertheless, the calculated particle size based on the capillary wave hypothesis is in reasonable agreement with the measured particle size, indicating the capillary wave mechanism in early stages of UVLD. The schematic of the capillary wave mechanism for the ejection of droplets from the melt pool in early stages of UVLD is presented in Fig. 6.

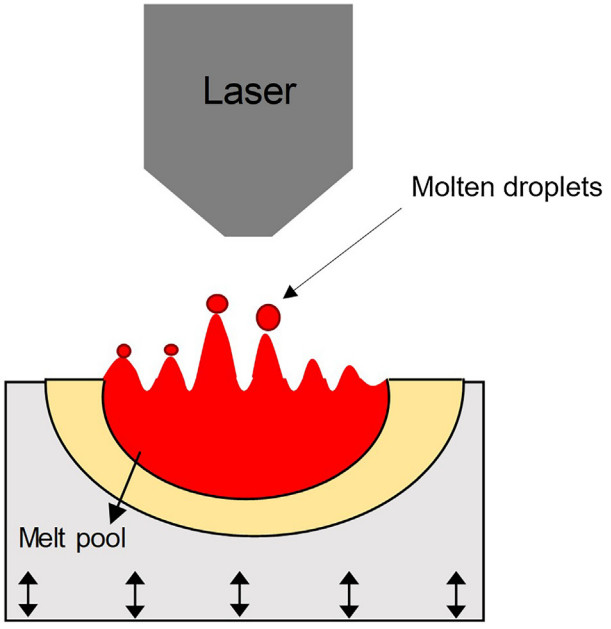

Fig. 6. Schematic of the capillary wave mechanism for the ejection of droplets from the melt pool in early stages of UVLD.

3.2. Geometrical and quality aspect of holes drilled with UVLD

The surface and cross-sectional SEM images of the holes drilled using UVLD for ultrasonic vibration displacements of 16, 24, and 32 μm at vibration frequencies of 20 and 40 kHz are presented in Fig. 7. The holes drilled with all the UVLD parameters exhibited good circularity at the entrance. The heat affected zone, indicated by the brighter contrast around the holes, becomes increasingly larger with increasing vibration displacement at both 20 and 40 kHz. The width of the heat affected zone was in the range of 400–700 μm. The surface of the specimens also show significant spatter due to deposition of ejected droplets. The spatter droplets are relatively bigger and more closely spaced near the hole rims. The holes drilled with higher vibration displacement (32 μm) also show significant buildup of material around the rim of the holes. The material build up is not uniform along the hole rims. The material

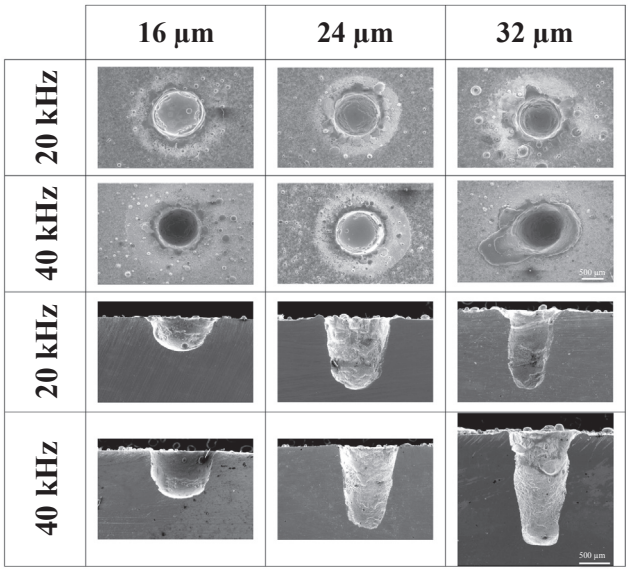

Fig. 7. Surface and cross-sectional SEM images of the laser drilled holes in AISI 316 steel for ultrasonic vibration displacements of 16, 24, and 32 μm at frequencies of 20 and 40 kHz.

build up is relatively distributed for holes drilled with 20 kHz while it is more pronounced on two sides of the hole for 40 kHz. The cross sectional SEM images show that the laser drilled holes were significantly tapered, especially the deeper holes drilled at higher vibration displacements. The ejected droplets during laser drilling also deposited and resolidified on the hole walls, resulting in rougher surface features on the inside walls of the holes. In general, the holes drilled with higher vibration displacements at each frequency show higher degree of surface deposition and re-solidification features. It was previously observed that the resolidified layers on the hole walls consisted of refined dendritic grains due to fragmentation of grains and upward flow of melt under the influence of ultrasonic vibrations for UVLD [25]. It was further shown that the thickness of resolidified layer actually decreases with increasing ultrasonic vibration displacement due to more efficient melt expulsion from the surfaces of holes.

The variation of hole depth and diameter with ultrasonic vibration displacement for vibration frequencies of 20 and 40 kHz is presented in Fig. 8. The results show that depending on laser processing and ultrasonic vibration parameters, the proposed UVLD process is capable of drilling sub-2 mm deep holes with diameter as small as 900 μm. While the diameter of the holes shows general decreasing trend, the depth of the hole increases almost linearly with the increasing ultrasonic vibration displacement for both 20 and 40 kHz. The diameters of the holes laser drilled with the vibration frequency of 20 kHz are slightly smaller than those drilled with the vibration frequency of 40 kHz especially at smaller ultrasonic vibration displacements (16 and 24 μm). The UVLD with higher ultrasonic vibration frequency (40 kHz) resulted in the formation of deeper and narrower holes. The ultrasonic vibration displacement has more pronounced effect on the geometric aspects (hole depth and diameter) of the drilled holes than the vibration frequency. For example, the doubling of vibration displacement from 16 to 32 μm resulted in about 124 and 143% increase in hole depth for 20 and 40 kHz, respectively. On the other hand, doubling the ultrasonic vibration frequency from 20 to 40 kHz resulted in about 24, 31, and 35% increase in hole depth for ultrasonic vibration displacements of 16, 24, and 32 μm, respectively. The effect of vibration frequency on the variation in diameter is much more pronounced at the lower vibration displacements (16 and 24 μm). The diameter of the laser drilled hole is about 930 μm for vibration displacement of 32 μm at both 20 and 40 kHz. The aspect ratio of the holes drilled with different ultrasonic

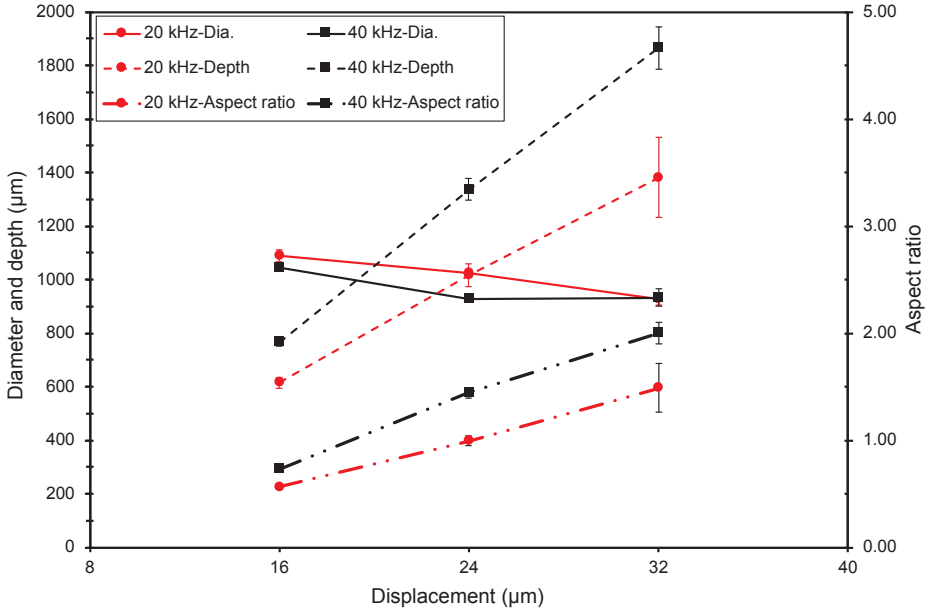

Fig. 8. Variation of the hole diameter, depth, and aspect ratio with vibration displacement for frequencies of 20 and 40 kHz during UVLD of AISI 316 steel.

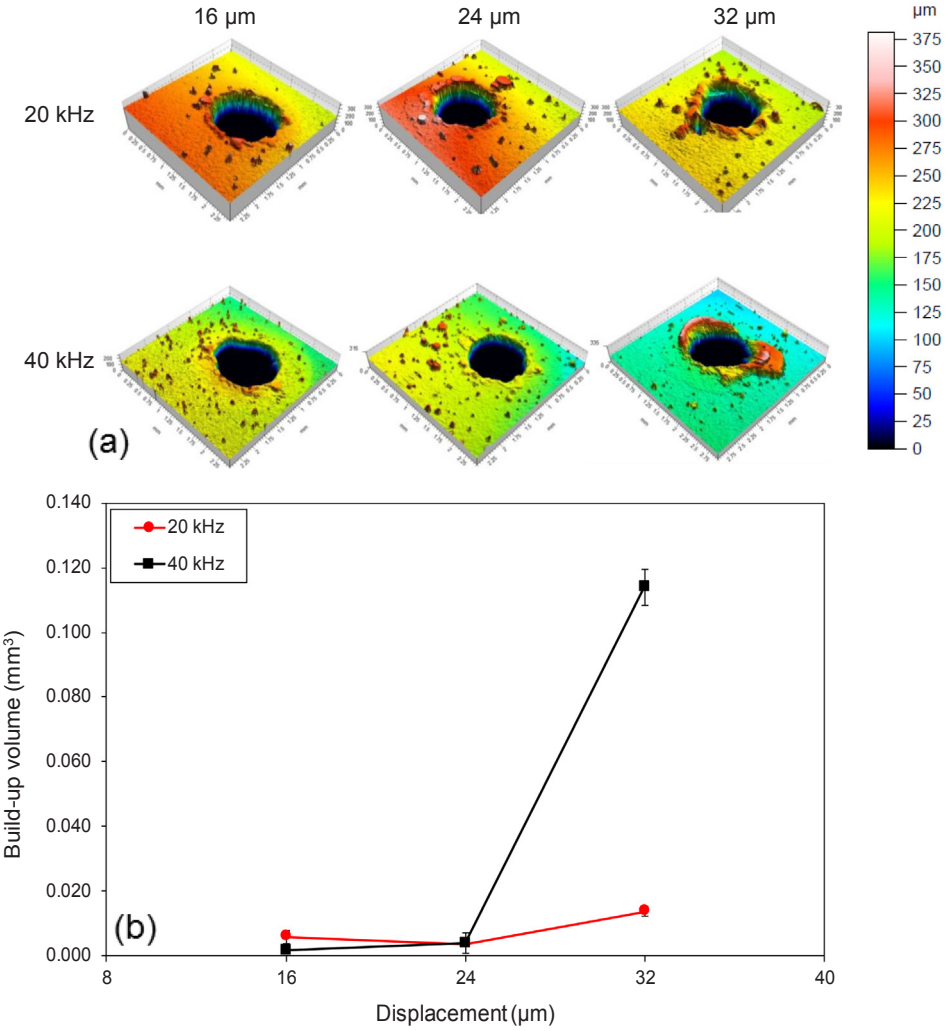

Fig. 9. (a) Three-dimensional surface profiles, and (b) Variation of volume of build-up material with vibration displacement for frequencies of 20 and 40 kHz during UVLD of AISI 316 steel.

parameters is also indicated in the Fig. 8. The highest aspect ratio of 2.0 was observed for the holes drilled with highest ultrasonic vibration displacement (32 μm) and vibration frequency (40 kHz) used in this investigation.

The increase in hole depth with increasing ultrasonic vibration displacement and frequency could be directly linked with the melt expulsion characteristics in early stages of drilling. Note that the high speed camera imaging showed that higher ultrasonic vibration frequency and displacement resulted in earlier initiation of droplet ejection, resulting in overall longer durations for material removal in the form of stream of ejected droplets and formation of deeper holes. The pronounced effect of ultrasonic vibration displacement is consistent for both the variation of droplet ejection initiation time and the hole depth. It was also observed that the entrance diameter of the holes decreases with increasing ultrasonic displacement and vibration frequency (Fig. 8). The SEM images also showed that holes become narrower, and hence tapered, with increasing depth of the holes (Fig. 7). The walls of the holes are also covered with deposited droplets and rims with build-up material for deeper holes. It appears that the reduction in diameter of the holes with increasing ultrasonic vibration displacement and frequency is directly correlated with the depth of the holes. Once the ejection of the droplets is initiated during the early stages of UVLD, the melt front advances downward and hole depth increases with continued laser irradiation. However, the complete ejection of droplets from the holes becomes increasingly difficult with increasing hole depth. The droplets ejected from deeper melt front impinge and re-solidify on the hole walls and near the rim as observed from the SEM images, causing an overall reduction in diameter of the holes. While droplet ejection is the dominant mechanisms of material removal during UVLD, it also appears that some vertical flow of molten material also contributes to material removal as observed from the layered build-up of material at the hole rims and deposition of material on the hole walls. The 3D surface profiles of the holes and measured volume of build-up material at the hole rims are presented in Fig. 9. In general, the build-up volume increases with increasing ultrasonic vibration displacement consistent with corresponding increase in depth of the holes. The volume of build-up area for holes drilled with lower ultrasonic displacement (16 and 24 μm) at both 20 and 40 kHz was less than 4×10^{-3} mm^3 (~0.2% of the total hole volume). However, a significant difference in build-up volume was observed for holes drilled with higher ultrasonic vibration displacement (32 μm). The volume of the build-up material for holes drilled with the vibration displacement of 32 μm was about 13.7×10^{-3} and 114×10^{-3} mm^3 for ultrasonic vibration frequency of 20 and 40 kHz, respectively. Clearly, the deeper holes are associated with larger build-up material due to difficulty in complete ejection of droplets and consequent deposition of droplets on the hole rims. Also, additional mechanism such as upward flow of molten material on the hole walls, especially for deeper holes, are likely to contribute to the build-up of material at the hole rims.

4. Conclusions

For UVLD of AISI 316 steel, the melt expulsion characteristics and geometric/quality features of the drilled holes were significantly influenced by ultrasonic vibration parameters (investigated frequencies of 20–40 kHz and displacements of 16–32 μm) for the given laser processing parameters. It was observed that increasing both ultrasonic vibration frequency and displacement resulted in earlier initiation of droplet ejection from the melt pool, resulting in the formation of deeper holes for the given laser irradiation time (100 ms). The effect of increasing ultrasonic vibration displacement was much more pronounced than the frequency on the reduction in droplet ejection initiation time and improvement in hole depth. The analysis of the solidified ejected droplets indicated the presence of capillary wave mechanism for droplet formation in the early stages of UVLD. The laser drilled holes, especially the deeper holes drilled with higher vibration frequency and displacement, were also associated with defects such as material build-up at on the hole walls and rims primarily due to incomplete ejection of droplets from deeper melt fronts. Further optimization of both laser processing and ultrasonic vibration parameters is likely to result in further improvements in geometric and quality aspects of the holes drilled using UVLD.

Acknowledgement

This material is based upon work supported by the National Science Foundation under Grant No. CMMI-1149079.

References

[1] S.S. Chang, G.M. Bone, Thrust force model for vibration-assisted drilling of aluminum 6061–T6, Int. J. Mach. Tools Manuf. 49 (2009) 1070–1076.
[2] S.S. Chang, G.M. Bone, Burr height model for vibration assisted drilling of aluminum 6061–T6, Precis. Eng. 34 (2010) 369–375.
[3] J. Pujana, A. Rivero, A. Celaya, L.L. de Lacalle, Analysis of ultrasonic-assisted drilling of Ti6Al4V, Int. J. Mach. Tools Manuf. 49 (2009) 500–508.
[4] T. Thoe, D. Aspinwall, M. Wise, Review on ultrasonic machining, Int. J. Mach. Tools Manuf. 38 (1998) 239–255.
[5] L. Balamuth, Ultrasonic assistance to conventional metal removal, Ultrasonics 4 (1966) 125–130.
[6] H. Xu, X. Jian, T.T. Meek, Q. Han, Degassing of molten aluminum A356 alloy using ultrasonic vibration, Mater. Lett. 58 (2004) 3669–3673.
[7] R.J. Lang, Ultrasonic atomization of liquids, J. Acoust. Soc. Am. 34 (1962) 6–8.
[8] S. Amini, M. Amiri, Study of ultrasonic vibrations' effect on friction stir welding, Int. J. Adv. Manuf. Technol. 73 (2014) 127–135.
[9] X. Liu, C. Wu, Elimination of tunnel defect in ultrasonic vibration enhanced friction stir welding, Mater. Des. 90 (2016) 350–358.
[10] T. Moriwaki, E. Shamoto, K. Inoue, Ultraprecision ductile cutting of glass by applying ultrasonic vibration, CIRP Ann.-Manuf. Technol. 41 (1992) 141–144.
[11] D.E. Brehl, T.A. Dow, Review of vibration-assisted machining, Precis. Eng. 32 (2008) 153–172.
[12] T. Watanabe, M. Shiroki, A. Yanagisawa, T. Sasaki, Improvement of mechanical properties of ferritic stainless steel weld metal by ultrasonic vibration, J. Mater. Process. Technol. 210 (2010) 1646–1651.
[13] H. Zheng, H. Huang, Ultrasonic vibration-assisted femtosecond laser machining of microholes, J. Micromech. Microeng. 17 (2007) N58.
[14] B. Kang, G.W. Kim, M. Yang, S.-H. Cho, J.-K. Park, A study on the effect of ultrasonic vibration in nanosecond laser machining, Opt. Lasers Eng. 50 (2012) 1817–1822.
[15] R. Dehoff, S. Babu, Characterization of interfacial microstructures in 3003 aluminum alloy blocks fabricated by ultrasonic additive manufacturing, Acta Mater. 58 (2010) 4305–4315.
[16] F. Ning, W. Cong, Microstructures and mechanical properties of Fe-Cr stainless steel parts fabricated by ultrasonic vibration-assisted laser engineered net shaping process, Mater. Lett. 179 (2016) 61–64.
[17] Y. Liao, Y. Chen, H. Lin, Feasibility study of the ultrasonic vibration assisted drilling of Inconel superalloy, Int. J. Mach. Tools Manuf. 47 (2007) 1988–1996.
[18] B. Azarhoushang, J. Akbari, Ultrasonic-assisted drilling of Inconel 738-LC, Int. J. Mach. Tools Manuf. 47 (2007) 1027–1033.
[19] M. Kadivar, J. Akbari, R. Yousefi, A. Rahi, M.G. Nick, Investigating the effects of vibration method on ultrasonic-assisted drilling of Al/SiCp metal matrix composites, Rob. Comput. Integr. Manuf. 30 (2014) 344–350.
[20] K. Alam, A. Mitrofanov, V.V. Silberschmidt, Experimental investigations of forces and torque in conventional and ultrasonically-assisted drilling of cortical bone, Med. Eng. Phys. 33 (2011) 234–239.
[21] W. Cong, F. Ning, A fundamental investigation on ultrasonic vibration-assisted laser engineered net shaping of stainless steel, Int. J. Mach. Tools Manuf. (2017).
[22] Y. Hu, F. Ning, W. Cong, Y. Li, X. Wang, H. Wang, Ultrasonic vibration-assisted laser engineering net shaping of ZrO_2-Al_2O_3 bulk parts: effects on crack suppression, microstructure, and mechanical properties, Ceram. Int. 44 (2018) 2752–2760.
[23] F. Ning, Y. Hu, Z. Liu, X. Wang, Y. Li, W. Cong, Ultrasonic vibration-assisted laser engineered net shaping of inconel 718 parts: microstructural and mechanical characterization, J. Manuf. Sci. Eng. 140 (2018) 061012.
[24] S. Biswas, S.H. Alavi, S.P. Harimkar, Laser surface melting of Ti–6Al–4V under the influence of ultrasonic vibrations, Mater. Lett. 159 (2015) 470–473.
[25] S.H. Alavi, S.P. Harimkar, Melt expulsion during ultrasonic vibration-assisted laser surface processing of austenitic stainless steel, Ultrasonics 59 (2015) 21–30.
[26] S.H. Alavi, S.P. Harimkar, Ultrasonic vibration-assisted continuous wave laser surface drilling of materials, Manuf. Lett. 4 (2015) 1–5.
[27] S.H. Alavi, S.P. Harimkar, Evolution of geometric and quality features during ultrasonic vibration-assisted continuous wave laser surface drilling, J. Mater. Process. Technol. 232 (2016) 52–62.
[28] S.H. Alavi, C. Cowell, S.P. Harimkar, Experimental and finite element analysis of ultrasonic vibration-assisted continuous wave laser surface drilling, Mater. Manuf. Processes (2016).
[29] M. Legay, N. Gondrexon, S. Le Person, P. Boldo, A. Bontemps, Enhancement of heat transfer by ultrasound: review and recent advances, Int. J. Chem. Eng. 2011 (2011).

[30] H.-Y. Kim, Y.G. Kim, B.H. Kang, Enhancement of natural convection and pool boiling heat transfer via ultrasonic vibration, Int. J. Heat Mass Transf. 47 (2004) 2831–2840.
[31] N.B. Dahotre, S. Harimkar, Laser Fabrication and Machining of Materials, Springer Science & Business Media, 2008.
[32] D. Sindayihebura, M. Dobre, L. Bolle, Experimental study of thin liquid film ultrasonic atomization, in: 4th World Conference on Experimental Heat Transfer, Fluid Mechanics and Thermodynamics, 1997, pp. 1249–1256.
[33] B. Vinet, J.-P. Garandet, B. Marie, L. Domergue, B. Drevet, Surface tension measurements on industrial alloys by the drop-weight method, Int. J. Thermophys. 25 (2004) 869–883.
[34] V. Bobkov, L. Fokin, E. Petrov, V. Popov, V. Rumiantsev, A. Savvatimsky, Thermophysical Properties of Materials for Nuclear Engineering: A Tutorial and Collection of Data, IAEA, Vienna, 2008.
[35] S.H. Alavi, S.P. Harimkar, Ultrasonic vibration-assisted laser atomization of stainless steel, Powder Technol. 321 (2017) 89–93.